

IMPROVED SIGNAL TREATMENT FOR CAPACITIVE LINAC PICKUPS

A. Reiter, C.-M. Kleffner, B. Schlitt, GSI, Germany

Abstract

For pulsed particle beams of linear accelerators capacitive pickups are a crucial diagnostic tool. In this contribution we present a simple, but effective time-domain analysis that has been established in various applications during several commissioning stages of two injector linacs. These injectors consist of a 400 keV/u radio-frequency quadrupole followed by a 7 MeV/u drift tube linac, both operated at 216.8 MHz. The main analysis objective was an improvement of the pulse shape reconstruction and, hence, of phase or energy determination.

INTRODUCTION

In the past years GSI has been involved in several projects in which new linear accelerators have come into operation. The medical therapy centres HIT and CNAO were equipped with a 216.8 MHz injector linac for the synchrotron consisting of a 400 keV/u radio-frequency quadrupole (RFQ) and a 7 MeV/u interdigital H-type drift tube linac (IH-DTL) [1, 2].

Operation frequencies above 200 MHz (periods $t_{rf} < 5$ ns) demand high-resolution diagnostics systems with GHz analogue bandwidth if higher harmonics are to be observed. Other practical problems can be encountered during measurements: electron field emission or secondary particles can significantly disturb pickup signals mounted close to a cavity and successive bunch signals tend to overlap at energies below 500 keV/u. Linac structures may be very susceptible to variations in operating parameters like rf amplifier phase and output power or cooling water temperature. In this experimental environment, we were forced to re-examine and to improve our existing analysis of pickup data.

In the next section we briefly describe pickup and data acquisition hardware, but emphasise the analysis procedure. Thereafter, experiment data and results are presented for RFQ and IH-DTL, respectively.

HARDWARE & DATA ANALYSIS

For the injectors of HIT and CNAO a pickup (in this paper also referred to as phase probe) acquisition and monitoring system was designed consisting of:

- phase probes (PHP) with inner radius $r = 31$ mm and 50Ω geometry ($f_{\text{Max}} < 3$ GHz)
- low-noise amplifiers (20-60 dB gain, 1 GHz analogue bandwidth)
- tank probes, i. e. inductive coupling loops, to monitor the rf fields in the cavities
- multi-channel ADC data acquisition system (8 bit, 4 GSa/s, 1 GHz bandwidth)

For the commissioning of each accelerator section a dedicated diagnostic test bench was set up with three phase

probes installed along a drift space [1, 2]. Some data were taken with a 5 GSa/s digital oscilloscope. For off-line analysis tank probe reference and all PHP signals were recorded. Three pickups guarantee the unambiguous determination of the bunch number that populates the drift space between any pair of phase probes. The mean kinetic bunch energy was determined via the well-known time-of-flight method.

Data Analysis

In two ways our analysis exploits the periodic nature of sampling process and acquired signals to improve detection sensitivity and effective timing resolution. The procedure for pulse shape reconstruction and energy determination can be summarised in five steps:

1. *In-pulse-average*: Raw data acquired within one macro-pulse are divided into blocks of length $N \cdot t_{rf}$ ($N=49$, t_{rf} = rf period) where the integer N is chosen such that all blocks start, within a tolerance < 5 ps, at a multiple of the sampling period $t_{DAQ}=250$ ps. At HIT, typically 10 blocks of 904 sample points are averaged calculating the sample mean to improve the signal-to-noise ratio.
2. *Interleaving*: The averaged data block is projected from N into one single rf period t_{rf} assigning to the k -th sample point the time $t(k) = \text{fmod}(k \cdot t_{DAQ}, t_{rf})$, the floating-point remainder of the ratio $k \cdot t_{DAQ}/t_{rf}$. At HIT, this compression enhances the timing resolution theoretically to about 5 ps.
3. *Post processing of waveforms*: FFT filter, moving average, smoothing or other algorithms
4. *Time offset t_{off} or phase relation* between signals: Determination of maximum position in the cyclic cross correlation of the two processed data sets. Here, we simply adopted the bin centre of the function maximum. At 216 MHz, a 5 ps timing resolution is equivalent to a 0.4° phase resolution.
5. *Energy calculation* via time-of-flight

The analysis parameters can be tailored to typical combinations of sampling and radio frequency. There are no free parameters – bunch number N_B , probe distance L , sampling and radio frequency are fixed. The estimates of the time t_{off} are very robust since all acquired samples are considered and a function with one local maximum is constructed. Therefore, the analysis procedure overcomes ambiguity problems of methods that arbitrarily choose “representative” signals to derive a single time offset, but disregard the majority of the data. A particularly inefficient example is the commonly used zero-crossing method which only considers the signal part around the base line and, unlike the cross correlation, is susceptible to DC offsets and drifts. Compared to other approaches we tested, data of poorer quality could still be analysed.

Model of Phase Probe Response

For signal calculations ref. [3] was adopted. The single-particle response [4] is fed into a phase probe modelled as RC circuit with $R = 50 \Omega$ and $C = 20 \text{ pF}$. The front-end amplifier was assumed to faithfully reproduce the input signal. Transmission effects along the coaxial cable were taken into account using the known cable attenuation. The output signal was folded with a uniform distribution of “effective bunch length” to describe the acquired data. This approach was chosen because the formula in ref. [4] was derived for a single on-axis particle by integration over the inner cylindrical surface, but particles with significant offset ($\sim r/3$) generate a narrower pulse of larger amplitude. The derivation in ref. [4] neglects the front ring of the phase probe that, in principle, is sensitive to the longitudinal electric field component, especially at the low energies ($\beta \ll 1$) considered here. Therefore, absolute signal amplitudes were not calculated and for comparison data had to be normalised. Despite its simplicity, the model delivered reasonable estimates of signal shape, bunch length and momentum spread.

Figure 1 shows calculated and measured phase probe signals for the 400 keV/u RFQ. The overlap of adjacent single-bunch responses (dashed lines) produces a significantly smaller, sine-like output signal (black line). After scaling of the signal amplitude, raw data sampled at 5 GSa/s (red dots) and reconstructed pulse shape after interleaving (blue) are in excellent agreement with the calculation. Note that the interleaved signal contains 1891 samples within 4.6 ns and no post processing was applied.

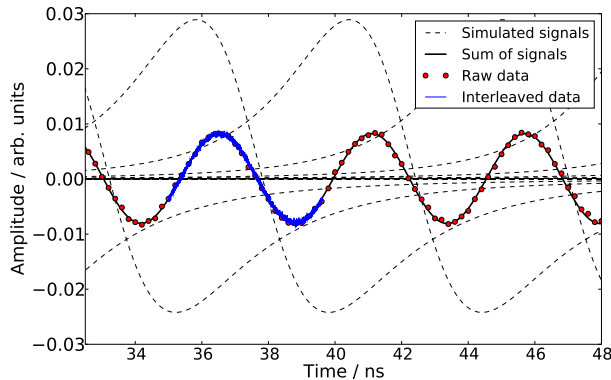


Figure 1: Signal comparison for a 400 keV/u RFQ beam.

If the response of the 75 m coaxial cable was omitted or the bunch length was changed in the calculation, only the signal amplitude was affected while the shape remained almost the same in line with experimental observations.

RFQ MEASUREMENTS

For the first time, a RFQ has been equipped with an internal re-buncher integrated into the tank [5, 6]. Re-buncher geometry and thus bunching voltage were mechanically adjusted to match energy and longitudinal focus of the RFQ beam to the IH-DTL input parameters. Without re-buncher, the RFQ energy gradually increases with rf power around the working point, with re-buncher

it slowly decreases. The correct operating point is found, if these two functions intersect at the IH-DTL injection energy [7]. Hence, it was important to map this energy dependence carefully over a large rf power range. With the new analysis we were able to extend the measurement range down to 80 % of the nominal rf power, where the RFQ starts to produce a bunched beam.

Longitudinal Focus Position

Three pickups PHP 1-3 were installed at distances of 361, 523 and 1128 mm from the re-buncher centre. The 1st accelerating gap of the IH-DTL was later at a position of 293 mm. When the operation parameters of the RFQ working point had been established, about 150 data samples were recorded at intervals of 30 seconds to monitor the stability. The samples are presented in fig. 2 (top), the mean energy is $(400.9 \pm 0.6) \text{ keV/u}$.

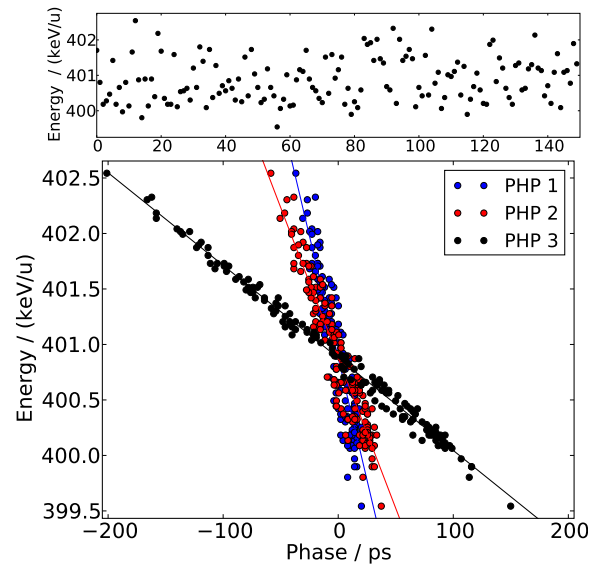


Figure 2: Trend of beam energy (top) and longitudinal phase space at three pickup positions (bottom).

Figure 2 (bottom) shows the measured beam energy as function of relative phase with respect to the mean value, defining the “reference bunch”. The phase values were derived for each data set from the measured time differences between tank reference and the three phase probe signals. Positive times correspond to bunches that are detected by a phase probe at a later time compared to the reference bunch. The increasing negative correlation of the distributions shows the expected divergent behaviour. The longitudinal focus of 287 mm behind the re-buncher centre was obtained by back-tracking of the distributions to the position where their correlations vanished. The close proximity to the 1st gap of the IH-DTL confirms the chosen re-buncher geometry.

The energy resolution $\sigma(E) \sim 0.06 \text{ keV/u}$ for the pair PHP 2 and 3 was calculated as standard deviation of the residuals between data and linear fit. Clearly, the much larger 0.6 keV/u (0.15 % mean energy) standard deviation of the shown energy distribution is not due to the data analysis. In fact, the closed-loop regulation controls the rf amplitude roughly to $\pm 0.2 \%$, a tolerance that could intro-

duce similar energy variations in the present case. Dark currents in the cavity identified during rf amplifier commissioning may also influence the system stability.

IH-DTL MEASUREMENTS

For the commissioning of the 7 MeV/u IH-DTL, the three phase probes were installed at much longer separations of 1148 and 2650 mm. Apart from the measured beam energy, estimates of effective bunch length and momentum spread were obtained on the basis of model calculations for the PHP signals.

Energy Loss Measurements

One important task of the pickup system is the monitoring of carbon stripping foils. Ten of these foils ($\sim 100 \mu\text{g}/\text{cm}^2$) are installed on a target ladder behind the IH-DTL.

Table 1: Comparison of energy loss data

Ion	$\Delta E(\text{th.})$	$\Delta E(\text{exp.})$	Comment
C	16.2 keV/u	(16.7 \pm 0.9) keV/u	all foils
p	5.4 keV	(6.0 \pm 0.4) keV	only 2 foils

At the beam energy of ~ 7 MeV/u, the measurement system achieves a short-term resolution $\sigma(E) \sim 0.4$ keV/u or $\sigma(E)/E \sim 6 \times 10^{-5}$, while over long periods further parameters must be monitored, e. g. a 1°C temperature change in the cooling water may shift the beam energy by up to 15 keV/u. The mean energy loss in each foil was determined from only 10 consecutive macro-pulses and calculated as energy difference with respect to a target-out reference measurement. Table 1 compares theoretical and measured energy losses. For the full set of foils the standard deviation of 0.9 keV/u is a measure of relative thickness uniformity at the time of installation, while the degradation of individual foils must be judged by comparison of repeated energy loss measurements.

Bunch Length and Momentum Spread

At the working point of the IH-DTL, the momentum spread $\Delta p/p$ of the beam reaches its minimum. At the same time, maximum PHP signal amplitudes are measured that significantly decrease, if the linac rf power is changed. The design value of $\Delta p/p$ is 0.2 %.

The phase probe signals of fig. 3 were acquired at a power level 5 % above the nominal value of ~ 900 kW, where their shapes indicate a large momentum spread. The interleaved signals (colours) were approximated with effective bunch lengths of 0.4, 0.8, and 1.8 ns, respectively. The uncertainty is of the order of 0.1 ns. The calculated signals are represented by black lines in fig. 3, the overall agreement is satisfactory. The discrepancy at the rising steep rising edge of PHP 1 might be due to the larger beam spot size or secondary particles since it is mounted directly behind the focussing quadrupole triplet. A realistic field calculation would have to include the full pickup geometry, especially the protective plates on both sides that suppress direct particle interactions.

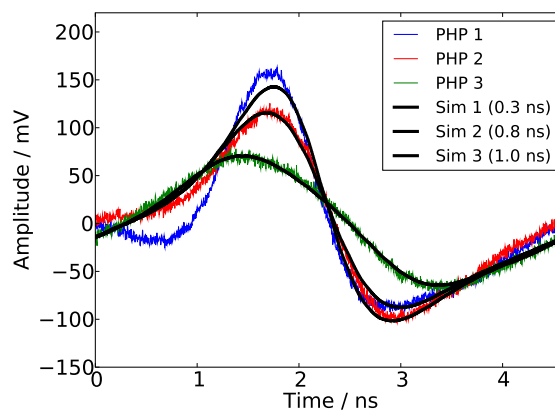


Figure 3: Comparison of measured and simulated pulse shapes for a 7.1 MeV/u H_3^+ beam at very high rf power

Plotting effective bunch length against phase probe distance, we extrapolated a reasonable bunch width of about 0.2 ns or $\Delta\phi = \pm 8^\circ$ at the IH-DTL exit from a straight-line fit. With this input value a one-dimensional, uniform particle distribution (line charge) was tracked along the drift space in a simulation. The bunch widths observed in fig. 3 were matched, when the momentum spread was set to 1.5 %. During standard operation, the signals of PHP 2 and 3 are almost identical with estimated effective bunch lengths of 0.8 and 1.0 ns, respectively. This is close to the resolution of the model calculation and the value $\Delta p/p = (0.2 \pm 0.1) \%$ must be considered as rough estimate of the momentum spread, despite the agreement with the design value.

CONCLUSIONS

A time-domain analysis has been tested successfully in various pickup applications. Timing offsets were monitored on a level of ~ 5 ps ($\sim 0.4^\circ$ phase at 217 MHz). Energy resolutions $\sigma(E)/E$ of 1.5×10^{-4} for a 400 keV/u RFQ beam and of 6×10^{-5} for a 7 MeV/u IH-DTL beam were achieved that allowed accurate energy measurements. The new signal reconstruction improved the system sensitivity and, together with a basic theoretical model, made rough estimates of bunch lengths or momentum spread possible.

REFERENCES

- [1] B. Schlitt, Proc. LINAC08, WE205, pp. 720-724, Victoria, BC, Canada
- [2] B. Schlitt et al., Proc. IPAC10, MOPEA003, pp. 67-69, Kyoto, Japan
- [3] S. R. Smith, SLAC-PUB-7244, July 1996, and references therein
- [4] P. Strehl, "Beam Instrumentation and Diagnostics", Springer, 2006
- [5] A. Bechthold et al., Proc. EPAC 2006, WEPCH117, p. 2191-2193, Edinburgh, Scotland, UK
- [6] A. Bechthold et al., Proc. PAC 2001, pp. 2485-2487, Chigaco, USA
- [7] C.-M. Kleffner et al., Proc. LINAC06, THP089, pp. 791-793, Knoxville, Tennessee, USA